



Published in final edited form as:

Cell Rep. 2021 April 20; 35(3): 109012. doi:10.1016/j.celrep.2021.109012.

## Hierarchical cell-type-specific functions of caspase-11 in LPS shock and antibacterial host defense

Puja Kumari<sup>1</sup>, Ashley J. Russo<sup>1</sup>, Skylar S. Wright<sup>1</sup>, Sureshkumar Muthupalani<sup>2</sup>, Vijay A. Rathinam<sup>1,3,\*</sup>

<sup>1</sup>Department of Immunology, UConn Health School of Medicine, 263 Farmington Ave., Farmington, CT 06030, USA

<sup>2</sup>Division of Comparative Medicine, Massachusetts Institute of Technology, Cambridge, MA 02139, USA

<sup>3</sup>Lead contact

### SUMMARY

Caspase-11 sensing of intracellular lipopolysaccharide (LPS) plays critical roles during infections and sepsis. However, the key cell types that sense intracellular LPS and their contributions to the host responses at the organismal level are not completely clear. Here, we show that macrophage/monocyte-specific caspase-11 plays a dominant role in mediating the pathological manifestations of endotoxemia, including gasdermin D (GSDMD) activation, interleukin (IL)-1 $\beta$ , IL-18, and damage-associated molecular pattern (DAMP) release, tissue damage, and death. Surprisingly, caspase-11 expression in CD11c<sup>+</sup> cells and intestinal epithelial cells (IECs) plays minor detrimental roles in LPS shock. In contrast, caspase-11 expression in neutrophils is dispensable for LPS-induced lethality. Importantly, caspase-11 sensing of intracellular LPS in LyzM<sup>+</sup> myeloid cells and MRP8<sup>+</sup> neutrophils, but not CD11c<sup>+</sup> cells and IECs, is necessary for bacterial clearance and host survival during intracellular bacterial infection. Thus, we reveal hierarchical cell-type-specific roles of caspase-11 that govern the host-protective and host-detrimental functions of the cytosolic LPS surveillance.

### Graphical abstract

---

This is an open access article under the CC BY-NC-ND license (<http://creativecommons.org/licenses/by-nc-nd/4.0/>).

\*Correspondence: rathinam@uchc.edu.

#### AUTHOR CONTRIBUTIONS

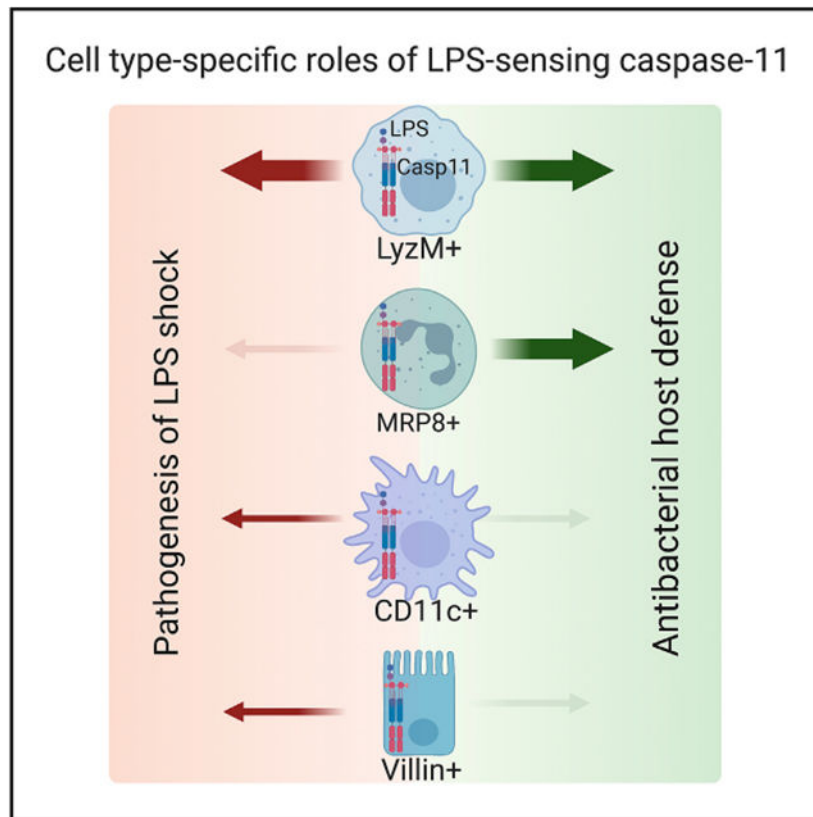
V.A.R. and P.K. conceived the study, designed the experiments, and wrote the manuscript. P.K. performed the experiments and analyzed the data. A.J.R. and S.S.W. provided technical help. S.M. performed the histopathological assessment of tissues.

#### DECLARATION OF INTERESTS

The authors declare no competing interests.

#### SUPPLEMENTAL INFORMATION

Supplemental information can be found online at <https://doi.org/10.1016/j.celrep.2021.109012>.



### In brief

Kumari et al. reveal hierarchical cell-type-specific roles of caspase-11 that govern the host-protective and host-detrimental functions of the cytosolic LPS surveillance pathway during bacterial infections and sepsis, respectively.

## INTRODUCTION

Intracellular sensing of bacterial lipopolysaccharide (LPS) is a critical surveillance mechanism during bacterial infections (Hagar et al., 2013; Kayagaki et al., 2013; Shi et al., 2014). A family of inflammatory caspases (caspase-11 in mice and caspase-4/5 in humans) sense LPS that gets access to the cytosol either through direct bacterial invasion or outer membrane vesicles (OMVs) (Shi et al., 2014; Vanaja et al., 2016). The lipid A moiety of LPS binds to the CARD domain of caspase-11, triggering the proteolytic activity of caspase-11. Active caspase-11, in turn, cleaves a pore-forming protein, gasdermin D (GSDMD), into two fragments (He et al., 2015; Kayagaki et al., 2015; Liu et al., 2016; Shi et al., 2015). GSDMD's N-terminal fragment (GSDMD-N) forms pores in the plasma membrane leading to  $K^+$  efflux, which activates the NLRP3 inflammasome-dependent maturation of caspase-1, IL-1 $\beta$ , and IL-18 (Kayagaki et al., 2015; Rühl and Broz, 2015; Schmid-Burgk et al., 2015). The plasma membrane disruption by GSDMD-N eventually leads to pyroptotic death of the cell and the release of intracellular molecules, such as HMGB1, IL-1 $\alpha$ , and the recently identified galectin-1, that act as alarmins or damage-

associated molecular patterns (DAMPs) to exacerbate inflammation (Kayagaki et al., 2011; Rathinam et al., 2019; Russo et al., 2021). Cytosolic LPS sensing by caspase-11 plays a protective role during bacterial infections (Aachoui et al., 2013; Wang et al., 2017a, 2017b, 2018). However, it also has the potential to cause tissue damage, disseminated intravascular coagulopathy (DIC), organ failure, and death (Kayagaki et al., 2011; Wu et al., 2019; Yang et al., 2019). Thus, cytosolic LPS sensing has multiple molecular outcomes and significant pathophysiological consequences.

Cytosolic LPS-sensing noncanonical inflammasome exists in a broader range of cell types. Several previous studies have shown that both hematopoietic and non-hematopoietic cells, including macrophages, dendritic cells (DCs), neutrophils, intestinal epithelial cells (IECs), airway epithelial cells, and endothelial cells, are competent for cytosolic LPS sensing (Chen et al., 2018; Cheng et al., 2017; Kayagaki et al., 2015; Knodler et al., 2014; Shi et al., 2014, 2015; Wang et al., 2018). The contributions of individual cell-type-specific cytosolic LPS sensing to the overall noncanonical inflammasome responses at the organismal level and, importantly, to pathophysiological manifestations of sepsis are emerging. It has recently been shown that caspase-11 expression in hepatocytes and endothelial cells also contributes to lethality during sepsis (Cheng et al., 2017; Deng et al., 2018).

Here, we comprehensively characterize monocyte/macrophage-, neutrophil-, DC-, and IEC-specific contributions of caspase-11 to the whole spectrum of host responses—GSDMD activation; pyroptosis; IL-1 $\beta$ , IL-18, and DAMP release; organ damage; and mortality—to cytosolic LPS using several *Casp11* conditional knockout (KO) mice. These *in vivo* studies showed that caspase-11 expression in monocytes/macrophages, and DCs to a lower extent, plays a dominant role in mediating pathophysiological manifestations of LPS shock, whereas neutrophil-intrinsic caspase-11's role in mediating LPS-induced lethality is negligible. Interestingly, IEC-intrinsic cytosolic sensing of LPS marginally contributes to the pathogenesis of LPS shock. In contrast, caspase-11 expression in monocytes/macrophages and neutrophils, but not DCs and IECs, plays a dominant protective role in the host defense against *Burkholderia thailandensis*, an intracellular bacterium. Collectively, our findings reveal the critical cellular compartments in which cytosolic LPS sensing operates to exert pathogenic inflammation as well as antibacterial host defense.

## RESULTS

### Macrophage/monocyte-intrinsic cytosolic LPS sensing drives lethal endotoxin shock

The excessive activation of caspase-11 by intracellular LPS eventually leads to death. Although caspase-11 can be activated in multiple cell types during LPS challenge, which cell-type-intrinsic cytosolic LPS sensing is responsible for the lethal consequence is not completely clear. To understand the contribution of myeloid compartment-specific caspase-11 to LPS-induced death, we deleted caspase-11 from monocytes/macrophages (*LyzM-cre<sup>+</sup>Casp11<sup>fl/fl</sup>*), neutrophils (*MRP8-cre<sup>+</sup>Casp11<sup>fl/fl</sup>*), and DCs (*Cd11c-cre<sup>+</sup>Casp11<sup>fl/fl</sup>*). *Casp11<sup>fl/fl</sup>*, *Casp11<sup>-/-</sup>*, and the conditional KO mice were challenged with LPS, and their survival was monitored. Consistent with previous findings, global *Casp11<sup>-/-</sup>* mice were highly resistant to the lethal LPS challenge (Figure 1A). Among the conditional KO strains, *LyzM-cre<sup>+</sup>Casp11<sup>fl/fl</sup>* survived significantly longer than *Casp11<sup>fl/fl</sup>* mice, and

*Cd11c-cre<sup>+</sup>Casp1<sup>fl/fl</sup>* survived longer than *Casp1<sup>fl/fl</sup>* mice but were less resistant than *LyzM-cre<sup>+</sup>Casp1<sup>fl/fl</sup>* mice to LPS shock (Figure 1A). Contrastingly, *MRP8-cre<sup>+</sup>Casp1<sup>fl/fl</sup>* mice were not protected from LPS-induced death (Figure 1B). In fact, *MRP8-cre<sup>+</sup>Casp1<sup>fl/fl</sup>* mice succumbed to death slightly earlier than *Casp1<sup>fl/fl</sup>* following LPS administration. IECs also express caspase-11 and are capable of intracellular LPS sensing (Knodler et al., 2014; Mandal et al., 2018). Furthermore, the coordinated action of caspase-11 with caspase-8 has been shown to cause intestinal damage during endotoxemia (Mandal et al., 2018). Nonetheless, whether cytosolic LPS sensing occurs in the IECs *in vivo* and whether it contributes to sepsis is unknown. To address this question, we deleted caspase-11 in IECs by crossing *Casp1<sup>fl/fl</sup>* mice with *Villin-cre<sup>+</sup>Casp1<sup>fl/fl</sup>* mice and subjected IEC-conditional KO mice to LPS shock. Interestingly, compared with the control mice, *Villin-cre<sup>+</sup>Casp1<sup>fl/fl</sup>* mice were slightly protected from the lethal dose of LPS. However, the difference is not statistically significant, and the protection in *Villin-cre<sup>+</sup>Casp1<sup>fl/fl</sup>* mice was of lower magnitude than that observed in *LyzM-cre<sup>+</sup>Casp1<sup>fl/fl</sup>* mice (Figure 1C). These results indicate that cytosolic LPS sensing in monocyte and macrophage compartments plays a major role in driving LPS-induced mortality with a minor contribution from that in the DC and IEC compartments.

### Tissue-dependent cell-type-specific contribution of caspase-11 to GSDMD, IL-1 $\beta$ , and IL-18 activation

To understand the cell-type-specific caspase-11 activity for GSDMD cleavage, we analyzed the activation status of GSDMD in the spleen and liver of naive and LPS-injected *Casp1<sup>fl/fl</sup>* and conditional KO mice. As expected, the spleen and liver of naive control and conditional KO mice had no GSDMD activation (Figure S1A). The control *Casp1<sup>fl/fl</sup>* mice that received LPS had a robust amount of GSDMD-N in the spleen and liver lysates (Figures 2A-2D and S1B-S1E). In contrast, we observed significantly reduced GSDMD cleavage in the spleen and liver of *LyzM-cre<sup>+</sup>Casp1<sup>fl/fl</sup>* and *Cd11c-cre<sup>+</sup>Casp1<sup>fl/fl</sup>* mice in comparison with *Casp1<sup>fl/fl</sup>* (Figures 2A-2D and S1B-S1E). However, there was no reduction in GSDMD cleavage in the spleen and liver of *MRP8-cre<sup>+</sup>Casp1<sup>fl/fl</sup>* mice (Figures 2C and 2D). This suggests that caspase-11 expression in monocytes/macrophages, as well as in DCs, is majorly responsible for the hepatic and splenic GSDMD cleavage during endotoxemia.

GSDMD membrane pore formation leading to K<sup>+</sup> ion efflux is considered to activate the NLRP3-inflammasome-mediated maturation and secretion of caspase-1, IL-18, and IL-1 $\beta$  (Kayagaki et al., 2015; Rühl and Broz, 2015; Schmid-Burgk et al., 2015). To characterize the role of caspase-11 expressed in various myeloid cells and IECs in the noncanonical inflammasome-dependent activation of IL-18 and IL-1 $\beta$ , we subjected the corresponding conditional KOs, along with the control mice, to LPS challenge and analyzed their plasma IL-18 and IL-1 $\beta$  profile. LPS-induced IL-18 and IL-1 $\beta$  secretion into the circulation was drastically reduced in *LyzM-cre<sup>+</sup>Casp1<sup>fl/fl</sup>* and *Cd11c-cre<sup>+</sup>Casp1<sup>fl/fl</sup>* (Figures 3A-3D). In contrast, IL-18 and IL-1 $\beta$  levels remained intact or reduced, respectively, in *MRP8-cre<sup>+</sup>Casp1<sup>fl/fl</sup>* mice (Figures 3C and 3D). Unlike in *LyzM-cre<sup>+</sup>Casp1<sup>fl/fl</sup>* and *Cd11c-cre<sup>+</sup>Casp1<sup>fl/fl</sup>* mice, there was no reduction in IL-18 and IL-1 $\beta$  levels in *Villin-cre<sup>+</sup>Casp1<sup>fl/fl</sup>* mice (Figures 3E and 3F).

In addition, we analyzed the cell-type-specific effect of caspase-11 on IL-18 response at the organ level. Compared with that in *Casp1<sup>fl/fl</sup>*, IL-18 levels in the spleen were reduced mainly in *LyzM-cre<sup>+</sup>Casp1<sup>fl/fl</sup>* mice (Figure 3G and 3H). In contrast, IL-18 levels in the liver were reduced only in *Cd11c-cre<sup>+</sup>Casp1<sup>fl/fl</sup>*, but not in *LyzM-cre<sup>+</sup>Casp1<sup>fl/fl</sup>* and *MRP8-cre<sup>+</sup>Casp1<sup>fl/fl</sup>* mice (Figures 3I and 3J). As expected, TLR4-dependent production of cytokines, such as IFN- $\beta$ , TNF, and IL-6, in caspase-11 conditional KO mice, including *LyzM-cre<sup>+</sup>Casp1<sup>fl/fl</sup>* and *Cd11c-cre<sup>+</sup>Casp1<sup>fl/fl</sup>*, were comparable with that of *Casp1<sup>fl/fl</sup>* mice (Figures 3K-3P). Furthermore, different myeloid cell populations, such as neutrophils, macrophages, and DCs, in the liver and spleen were comparable among LPS-injected *Casp1<sup>fl/fl</sup>* and conditional KO mice (Figure S2). Considering the crosstalk among cell death pathways (Snyder and Oberst, 2021), we assessed the activation status of other cell death pathways, such as apoptosis and necroptosis, in caspase-11 conditional KO mice. LPS challenge did not lead to MLKL activation, a proxy for necroptosis, in *Casp1<sup>fl/fl</sup>* and caspase-11 conditional KO mice (Figure S3). Furthermore, caspase-3 cleavage, a marker of apoptosis, was found to be comparable among all the genotypes tested (Figure S3). These data rule out a compensatory activation of other cell death pathways in LPS-injected caspase-11 conditional KO mice.

### Macrophage/monocyte-intrinsic cytosolic LPS sensing mediates DAMP release during endotoxemia

In addition to promoting the activation and release of pro-inflammatory cytokines IL-1 $\beta$  and IL-18 through GSDMD pores, cytosolic LPS sensing also causes the release of DAMPs and alarmins, such as IL-1 $\alpha$  and HMGB1. The DAMPs and alarmins are mostly intracellular proteins under the resting state but released to the extracellular space as a result of the plasma membrane disruption during lytic cell death. These DAMPs and alarmins play critical roles in propagating pathological inflammation and often contribute to sepsis mortality. We recently discovered galectin-1, a  $\beta$ -galactoside-binding lectin, as a DAMP/alarmin released due to canonical and noncanonical inflammasome-driven pyroptosis, as well as necroptosis (Russo et al., 2021). Galectin-1 amplifies the inflammatory responses and lethality during endotoxemia. To understand the cell-type-specific role of caspase-11 in inducing DAMP release during endotoxin shock, we challenged various caspase-11 conditional KO mice and the corresponding control mice with LPS and analyzed the plasma levels of DAMPs, such as IL-1 $\alpha$ , HMGB1, and galectin-1. The release of IL-1 $\alpha$ , HMGB1, and galectin-1 into the circulation was substantially reduced in *LyzM-cre<sup>+</sup>Casp1<sup>fl/fl</sup>* mice compared with *Casp1<sup>fl/fl</sup>* mice (Figures 4A-4C). The plasma levels of IL-1 $\alpha$  and HMGB1, but not galectin-1, were reduced in *Cd11c-cre<sup>+</sup>Casp1<sup>fl/fl</sup>* mice (Figures 4D-4F). *Villin-cre<sup>+</sup>Casp1<sup>fl/fl</sup>* mice also had reduced circulating levels of HMGB1 and galectin-1, but not IL-1 $\alpha$  (Figures 4G-4I). The plasma levels of IL-1 $\alpha$ , HMGB1, and galectin-1 remained unchanged in *MRP8-cre<sup>+</sup>Casp1<sup>fl/fl</sup>* mice (Figures 4D-4F), which contrasts with the observations in *LyzM-cre<sup>+</sup>Casp1<sup>fl/fl</sup>*, *Cd11c-cre<sup>+</sup>Casp1<sup>fl/fl</sup>*, and *Villin-cre<sup>+</sup>Casp1<sup>fl/fl</sup>* mice. In summary, of the cell types analyzed, intracellular LPS sensing in monocytes/macrophages maximally contributes to the DAMP release during endotoxemia.

## Caspase-11 expression in various myeloid cells differentially contributes to cytosolic LPS-induced tissue damage

Cytosolic LPS-elicited responses can also lead to tissue damage and organ pathology, principal pathophysiological manifestations of septic shock (Cheng et al., 2017). We next assessed the contribution of caspase-11 expressed in different cellular compartments to LPS-induced tissue damage and organ pathology. Unlike naive mice, LPS-injected *Casp1<sup>fl/fl</sup>* mice had multifocal to coalescing, random, well-demarcated foci of hepatocellular degeneration (cell swelling, cytoplasmic clearing) with a few scattered necrotic hepatocytes (hypercarnophilic hepatocytes with karyolysis) and occasional single-cell necrosis in the liver (Figures 5A, 5B, and S4). Mild-to-moderate venous and sinusoidal congestion was frequently noted in the *Casp1<sup>fl/fl</sup>* liver (Figures 5A and 5B). Furthermore, low numbers of neutrophils and macrophages were seen within necrotic foci and multifocally within the perisinusoidal spaces in the liver of *Casp1<sup>fl/fl</sup>* mice (Figures 5A and 5B). These histopathological changes were drastically reduced in the livers of *LyzM-cre<sup>+</sup>Casp1<sup>fl/fl</sup>* and *MRP8-cre<sup>+</sup>Casp1<sup>fl/fl</sup>* mice, but not in *Cd11c-cre<sup>+</sup>Casp1<sup>fl/fl</sup>* mice (Figures 5A, 5B, and S4). As a proxy for organ damage, circulating levels of organ damage markers, such as aspartate aminotransferase (AST), alanine aminotransferase (ALT), and lactate dehydrogenase (LDH), were also measured in the plasma of *Casp1<sup>fl/fl</sup>*, *LyzM-cre<sup>+</sup>Casp1<sup>fl/fl</sup>*, *MRP8-cre<sup>+</sup>Casp1<sup>fl/fl</sup>*, and *Cd11c-cre<sup>+</sup>Casp1<sup>fl/fl</sup>* mice administered with LPS. Whereas *Casp1<sup>fl/fl</sup>* mice had high plasma levels of AST, ALT, and LDH, *LyzM-cre<sup>+</sup>Casp1<sup>fl/fl</sup>* mice had significantly reduced levels of AST and LDH (Figures 5C-5E and S4). AST, but not ALT and LDH, levels were reduced in *MRP8-cre<sup>+</sup>Casp1<sup>fl/fl</sup>* mice. AST, ALT, and LDH levels in *Cd11c-cre<sup>+</sup>Casp1<sup>fl/fl</sup>* were comparable with that of *Casp1<sup>fl/fl</sup>* mice. It is evident from these data that intracellular LPS sensing in *LyzM<sup>+</sup>* monocytes/macrophages is involved in inducing organ damage during endotoxin shock.

## Cytosolic LPS sensing in *LyzM<sup>+</sup>* myeloid cells and *MRP8<sup>+</sup>* neutrophils, but not DCs and IECs, is necessary for the host survival during an intracellular bacterial infection

The cytosolic LPS sensing pathway is a double-edged defense arsenal; although its excessive activation has lethal consequences, it plays a vital role in protecting the host from bacterial infections (Rathinam et al., 2019; Russo et al., 2018). *B. thailandensis* is an intracellular Gram-negative bacterium, which escapes from the phagosome to replicate in the cytosol (Wiersinga et al., 2006). Caspase-11 sensing of *B. thailandensis* LPS is crucial to the host resistance; *caspase-11<sup>-/-</sup>* mice succumb to even a low-dose *B. thailandensis* infection, whereas WT mice robustly control the infection (Aachoui et al., 2015). Having identified the cell-type-specific detrimental role of caspase-11 in LPS-induced shock, we next explored the cell-type-specific protective role of caspase-11 in antibacterial host defense by using *B. thailandensis* as a model organism. For this, we infected *Casp1<sup>fl/fl</sup>*, *Casp11<sup>-/-</sup>*, and the conditional KO mice intraperitoneally with  $10^3$  colony-forming units (CFUs) of *B. thailandensis* and monitored their survival. All the *Casp1<sup>fl/fl</sup>* mice survived for up to 30 days post-infection, whereas *Casp11<sup>-/-</sup>* mice failed to survive beyond 4–5 days. Importantly, *LyzM-cre<sup>+</sup>Casp1<sup>fl/fl</sup>* and *MRP8-cre<sup>+</sup>Casp1<sup>fl/fl</sup>* mice succumbed to *B. thailandensis* infection within 5–7 days and 7–11 days, respectively (Figure 6A). Interestingly, *Cd11c-cre<sup>+</sup>Casp1<sup>fl/fl</sup>* and *Villin-cre<sup>+</sup>Casp1<sup>fl/fl</sup>* mice survived just like *Casp1<sup>fl/fl</sup>* mice upon *B. thailandensis* infection (Figure 6A). These data clearly show that the cytosolic sensing of *B.*

*thailandensis* by caspase-11 in monocytes/macrophages and neutrophils is essential for host survival.

### Cytosolic LPS sensing in LyzM<sup>+</sup> myeloid and MRP8<sup>+</sup> neutrophil compartments mediates bacterial clearance during *B. thailandensis* infection

We next assessed the cell-type-specific role of caspase-11 in bacterial clearance during *B. thailandensis* infection. *Casp11<sup>fl/fl</sup>*, *Casp11<sup>-/-</sup>*, and the conditional KO mice were infected with 10<sup>3</sup> CFUs of *B. thailandensis*, and the bacterial burden in the spleen and liver 3 days post-infection was measured. *Casp11<sup>fl/fl</sup>* mice had an undetectable bacterial load, whereas *Casp11<sup>-/-</sup>* mice had a high bacterial burden in their spleen and liver (Figures 6B and 6C). More importantly, *LyzM-cre<sup>+</sup>Casp11<sup>fl/fl</sup>* and *MRP8-cre<sup>+</sup>Casp11<sup>fl/fl</sup>* mice, like *Casp11<sup>-/-</sup>* mice, failed to control bacterial replication as their spleen and liver harbored higher numbers of bacteria (Figures 6B and 6C). Interestingly, the comparison of bacterial loads among these three strains of mice revealed that *Casp11<sup>-/-</sup>* mice had the highest bacterial load, followed by *LyzM-cre<sup>+</sup>Casp11<sup>fl/fl</sup>* and *MRP8-cre<sup>+</sup>Casp11<sup>fl/fl</sup>* mice, which had intermediate and lower bacterial loads, respectively. Thus, bacterial loads in these mice mirrored their survival. Noticeably, all *MRP8-cre<sup>+</sup>Casp11<sup>fl/fl</sup>* mice fail to control bacterial burden in the spleen, whereas a few *MRP8-cre<sup>+</sup>Casp11<sup>fl/fl</sup>* mice were able to clear bacteria from the liver (Figure 6C). These data indicate an organ-specific role of neutrophil caspase-11 and may explain the relatively more prolonged survival of *MRP8-cre<sup>+</sup>Casp11<sup>fl/fl</sup>* mice than *Casp11<sup>-/-</sup>* and *LyzM-cre<sup>+</sup>Casp11<sup>fl/fl</sup>* mice. In contrast with *Casp11<sup>-/-</sup>*, *LyzM-cre<sup>+</sup>Casp11<sup>fl/fl</sup>*, and *MRP8-cre<sup>+</sup>Casp11<sup>fl/fl</sup>* mice, *Cd11c-cre<sup>+</sup>Casp11<sup>fl/fl</sup>* mice cleared bacteria in both liver and spleen. Overall, caspase-11-dependent intracellular LPS sensing in monocytes/macrophages and neutrophils, but not in DCs, plays an essential role in bacterial clearance and host protection during *B. thailandensis* infection (Figure 6D).

## DISCUSSION

Cytosolic LPS sensing through inflammatory caspases, such as caspase-4/11, is considered a key mechanism of innate immune activation during Gram-negative bacterial infections (Rathinam et al., 2019). Various immune and nonimmune cells, such as monocytes, macrophages, DCs, neutrophils, IECs, airway epithelial cells, and endothelial cells, express caspase-4/11 and GSDMD, and thus are competent for cytosolic LPS sensing *in vitro* (Chen et al., 2018; Cheng et al., 2017; Kayagaki et al., 2015; Knodler et al., 2014; Shi et al., 2014, 2015; Wang et al., 2018). However, whether these cells participate in cytosolic LPS sensing *in vivo* and the extent to which they contribute to host defense and various pathophysiological manifestations during septic shock are not wholly known. Our results demonstrate differential contributions of monocyte/macrophage-, DC-, neutrophil-, and IEC-specific caspase-11 to a spectrum of intracellular LPS-elicited host responses.

Of all the cellular compartments examined in this study, cytosolic LPS sensing in LyzM<sup>+</sup> myeloid cells, such as macrophages and monocytes, plays a dominant role in eliciting GSDMD-dependent pyroptosis, IL-1 $\beta$  and IL-18 activation, and the DAMP release at the organismal level during systemic LPS exposure. Furthermore, pathological manifestations, such as organ damage and mortality during LPS shock, are also mediated by macrophage/

monocyte-intrinsic caspase-11. Nonetheless, our data suggest that cytosolic LPS sensing in additional non-myeloid cell types also contributes to LPS-induced lethality. Consistent with this, it has been shown that endothelial expression of caspase-11 and sensing of LPS plays a vital role in endotoxemia; specifically, caspase-11-mediated pyroptosis of endothelial cells induced acute lung injury and mortality (Cheng et al., 2017). Furthermore, Deng et al. (2018) have demonstrated that the hepatocyte-specific deletion of caspase-11 reduced the release of HMGB1 and IL-1 $\alpha$  and mortality in mice subjected to LPS challenge. Considering that myeloid-specific deletion of caspase-11 in this study and endothelial- and hepatocyte-specific deletion of caspase-11 (Cheng et al., 2017; Deng et al., 2018) rescued approximately 50%–60% of mice from LPS shock, it is evident that intracellular LPS sensing in these three cell types is a significant driver of LPS-induced lethality. Also emerging from our studies is minor roles for DC- and IEC-specific caspase-11 in endotoxin shock. Collectively, these findings emphasize not just the existence of the noncanonical inflammasome in many hematopoietic and nonhematopoietic cell types but also, more importantly, their critical contributions to pathological outcomes of exposure to excessive LPS.

Interestingly, despite their comparable contributions to splenic and hepatic GSDMD cleavage, macrophage-caspase-11 and DC-caspase-11 have different effects on survival and organ damage. The ESCRT-mediated repair of the plasma membrane, perforated by GSDMD pores, is an important factor that determines the extent of cell death downstream of GSDMD cleavage (Rühl et al., 2018). DCs have also been shown to undergo minimal pyroptosis and become hyperactive when stimulated with specific inflammasome triggers such as oxidized lipids (Zanoni et al., 2016). Considering many cell biological differences between DCs and macrophages, the cytoprotective mechanisms, such as ESCRT repair, may be more efficient in DCs than in macrophages. As a result of which, despite the similar level of GSDMD activation in DCs and macrophages, the downstream pyroptosis and DAMP release, which are key mechanisms driving organ damage and death, likely occur at a higher rate in macrophages.

Our comparative analysis in *B. thailandensis* infection and endotoxemia models uncovered differential cell-type-specific roles of caspase-11 in antibacterial protection versus lethal inflammation; caspase-11 sensing of LPS in LyzM<sup>+</sup> myeloid cells plays a more critical role in antibacterial host defense than in lethal endotoxemia. The role of neutrophil-intrinsic caspase-11 is also found to be different during bacterial infections versus endotoxemia. Emerging literature shows neutrophils express canonical inflammasome components and are capable of secreting IL-1 $\beta$  and IL-18 and undergoing pyroptotic cell death (Chen et al., 2014; Karmakar et al., 2020; Mankan et al., 2012; Nichols et al., 2017; Sollberger et al., 2018). The noncanonical inflammasome is also functional in neutrophils, the activation of which triggers pyroptosis and neutrophil extracellular traps (NETs) formation *in vitro* (Chen et al., 2018). Our data provide genetic evidence that neutrophil-intrinsic sensing of intracellular LPS is vital for bacterial control and host survival during *B. thailandensis* infection, which is consistent with a recent study (Kovacs et al., 2020).

In contrast, neutrophil-intrinsic caspase-11 plays a minor role during endotoxin shock, which contrasts with the reduced susceptibility of mice lacking caspase-11 in other myeloid

compartments, such as macrophages/monocytes. A few possibilities may account for the differential role of neutrophil-intrinsic caspase-11 in LPS shock versus *B. thailandensis* infection. The magnitudes of caspase-11 activation in neutrophils during LPS shock and *B. thailandensis* infection may differ; cytosolic LPS sensing may occur only at a negligible level in neutrophils during LPS shock. Conversely, following *B. thailandensis* invasion of the cytosol, LPS concentration inside neutrophils likely reaches a threshold sufficient for robust caspase-11 activation and pyroptosis (Kovacs et al., 2020). In addition, cytosolic LPS sensing in neutrophils during LPS shock may be redundant with other cell types, such as macrophages, monocytes, and endothelial cells. However, neutrophils are an indispensable cell type in bacterial clearance and host protection against *Burkholderia* infection. Whereas caspase-1 activation by canonical inflammasomes is a poor inducer of neutrophil pyroptosis, caspase-11 activation by LPS is a potent activator (Chen et al., 2018; Karmakar et al., 2020; Kovacs et al., 2020). Accumulating evidence from the recent reports suggests that caspase-11-dependent pyroptosis of neutrophils via GSDMD is necessary for the host to clear *B. thailandensis* infection (Kovacs et al., 2020; Wang et al., 2019). The mechanisms by which neutrophil pyroptosis confers host protection against *B. thailandensis* are yet to be identified.

The endotoxemia model used in this study has limitations in simulating pathophysiological manifestations of the infection-triggered human sepsis. However, it was used for its utility in displaying the pathological outcomes of excessive activation of the caspase-11 pathway. It should also be noted that cre-based conditional deletion relies on the expression of specific genes in specific cell types. However, certain genes can be expressed in additional cell types; for instance, *LyzM*, *MRP8*, and *Cd11c* that are being used as lineage-specific markers could be expressed in other cell types as reported previously (Abram et al., 2014). As a result, the inadvertent deletion of molecules in such non-target cell types is possible and should be taken into consideration in the interpretation of data obtained using cre-expressing strains. Despite this drawback, the cre-lox method remains the best genetic approach to study the cell-type-specific functions of molecules and pathways. In our study, the phenotype (protection from LPS shock) observed in *LyzM-cre<sup>+</sup>Casp11<sup>fl/fl</sup>* mice is most likely due to *Casp11* deletion in macrophages/monocytes and least likely due to deletion in neutrophils because *LyzM-cre<sup>+</sup>Casp11<sup>fl/fl</sup>* and *MRP8-cre<sup>+</sup>Casp11<sup>fl/fl</sup>* mice did not phenocopy each other. Similarly, the phenotype observed in *Cd11c-cre<sup>+</sup>Casp11<sup>fl/fl</sup>* mice is least likely due to deletion in macrophages/monocytes because *Cd11c-cre<sup>+</sup>Casp11<sup>fl/fl</sup>* and *LyzM-cre<sup>+</sup>Casp11<sup>fl/fl</sup>* mice showed contrasting phenotypes upon *B. thailandensis* infection. In summary, by generating several cell-type-specific conditional KO mice, we delineate the precise role of cytosolic LPS sensing in multiple cell types during endotoxemia and intracellular bacterial infection.

## STAR★METHODS

### RESOURCE AVAILABILITY

**Lead contact**—Further information and requests for resources and reagents should be directed to and will be fulfilled by the Lead Contact, Vijay Rathinam (rathinam@uchc.edu).

**Materials availability**—Mouse lines generated in this study will be shared by the Lead Contact (subject to their availability at the time of request).

**Data and code availability**—This study did not generate any unique datasets or code.

## EXPERIMENTAL MODEL AND SUBJECT DETAILS

Casp11<sup>fl/fl</sup> mice, a kind gift of Dr. Vishva Dixit, was bred at UConn Health. *Lyz2-cre*, *MRP8-cre-ires/GFP*, *Cd11c-cre* (Itgax-cre), and *Villin-cre* (Vil1-cre) mice were obtained from The Jackson Laboratory (Bar Harbor, ME) and bred with *Casp11<sup>fl/fl</sup>* mice at UConn Health to generate the respective conditional knockout mice. All mice were maintained in specific pathogen-free conditions in the animal facilities of UConn Health. The animal protocols were carried out in accordance with the guidelines set forth by the UConn Health Institutional Animal Care and Use Committee. Age- and sex-matched male and female mice (not co-housed) of 8–24 weeks old were used. Non-littermate *Casp11<sup>fl/fl</sup>* mice were used as controls. Genotyping for the *caspase-11* allele was performed as described previously with the primers CCCTGGAAAAATCGATGACT, TGAAATGCATGTACTGAGAGCAAGG, and CAATTGACTTGGGGATTCTGG. Genotyping for *LyzM-cre* was performed with CCCAGAAATGCCAGATTACG, CTTGGGCTGCCAGAATTTCTC, and TTACAGTCGGCCAGGCTGAC. Genotyping for *MRP8-cre-ires/GFP* was performed with the primers GCGGTCTGGCAGTAAAACTATC, GTGAAACAGCATTGCTGTCACTT, CTAGGCCACAGAATTGAAAGATCT, and GTAGGTGGAAATTCTAGCATCATCC. Genotyping for *Cd11c-cre* was performed with the primers ACTTGGCAGCTGTCTCCAAG, GCGAACATCTTCAGGTTCTG, CAAATGTTGCTTGTCTGGTG, and GTCAGTCGAGTGCACAGTTT. Genotyping for *Villin-cre* was performed with the primers GCTTTCAAGTTTCATCCATGTTG, TTCATGATAGACAGATGAACACAGT, and GTCTTTGGGTAAAGCCAAGC.

## METHOD DETAILS

**Survival studies**—*Escherichia coli* O111:B4 LPS (20 mg/kg; Sigma) was injected intraperitoneally, and the survival of the mice was observed for five days. In separate studies, mice were injected intraperitoneally with 10<sup>3</sup> CFU of mouse-passaged *B. thailandensis* E264-1 strain (Aachoui et al., 2015), and the survival of mice was observed for 30 days.

**Cytokine analysis and Immunoblotting**—Plasma, spleen, and liver from mice were harvested 8 h post-LPS injection. Organs were harvested in PBS containing 1x protease inhibitor, homogenized with homogenizer 150 (Fisherbrand). Mature IL-1 $\alpha$  and IL-1 $\beta$ , TNF, and IL-6 were analyzed by ELISA kits (Thermo Scientific Fisher) according to the manufacturer's protocol. IL-18 levels were assessed as previously described (Banerjee et al., 2018) using a mature IL-18-specific ELISA with antibodies from MBL (Fang et al., 2019; Flood et al., 2019; Kovacs et al., 2020; Liu et al., 2012; Nichols et al., 2017). IFN- $\beta$  levels were assessed by ELISA as previously described (Banerjee et al., 2018). HMGB1 levels were detected with an IBL international ELISA Kit (#ST51011) according to the manufacturer's protocol. Galectin-1 levels were measured using the R&D ELISA kit (#DY1245) as described previously (Russo et al., 2021). Total protein was quantified with a BCA assay kit (Pierce BCA Protein Assay Kit; #23227). Fifty  $\mu$ g

of total protein was used for SDS-PAGE and immunoblotting. Samples were added to NuPAGE LDS sample buffer (Invitrogen), run on polyacrylamide gels, and then transferred onto nitrocellulose membranes using the Trans-Blot Turbo Transfer System (Bio-Rad). Membranes were blocked in 2.5% milk and probed with the appropriate primary and secondary antibodies. Blots were visualized for proteins using the Bio-Rad Clarity-ECL HRP substrate (#102031510 and #102031511) on a Syngene gel documentation box. Immunoblot analysis was done with antibodies to mouse GSDMD (#Ab209845), caspase-11 (Cell Signaling, #14340S), MLKL (Cell Signaling, #37705S), pMLKL (Cell Signaling, #37333S), caspase-3 (Cell Signaling, #9664S), GAPDH (Cell Signaling, #5174), and  $\beta$ -actin (Cell Signaling, #3700).

**Flow cytometry**—*Casp11<sup>fl/fl</sup>*, *Casp11<sup>-/-</sup>*, and the conditional KO mice were either injected with PBS or 20 mg/kg LPS for 4 h. Liver and spleen were harvested, finely chopped and incubated in 25 mL of digestion buffer [150U/ml collagenase (Sigma Aldrich, #C5138-5G), 60 U/ml DNase I (Sigma Aldrich, #DN25-1G), 2% FBS, 1 mM CaCl<sub>2</sub>, and 1 mM MgCl<sub>2</sub> in BSS] for 30 min (spleen) or 45 min (liver) at 37°C with shaking (445 RPM). Then 25 mL of 1 mM EDTA in BSS was added to the tubes, and the tubes were centrifuged at 4°C for 5 min at 350 xg, and the supernatant was discarded. RBCs in the cell pellet were lysed with 2-3 mL of ACK lysis buffer (Lonza, #10-548E) for ~1-5 min. Finally, cells were resuspended in 1 mL of FACS buffer (PBS, 2% FBS, 1mM EDTA 0.5 M, pH 7.4, 0.1% NaN<sub>3</sub>) and blocked with 100  $\mu$ L of Fc block (1:60 dilution in FACS buffer) for 20 min at 4°C. Cells were spun as mentioned above and the supernatant was removed before staining with the following antibodies for cell surface markers (1:200 dilution, for 20 min at 4°C): anti-Cd11b-APC (BioLegend, #101212), Cd11c-PE/Cy7 (BioLegend, #117318), Ly6C-PerCPCy5.5 (BioLegend, #128012), Ly6G-Pac blue (BioLegend, #127612), F4/80-PE (BioLegend, #123110), B220-AF700 (BioLegend, #103232), CD3-AF700 (BioLegend, #152316), and UV-Blue live dead (Invitrogen, #L34962). Cells were then fixed with 1.5% formaldehyde for 30 min at 4°C. Cells were washed, resuspended in FACS buffer, and subjected to analysis in BD LSR II. FACS data were analyzed with Flow Jo version 10.7.

**Organ damage analysis**—Mice were injected intraperitoneally with 20 mg/kg LPS. Blood and liver were harvested 16 h post LPS injection for organ damage marker and histopathology analysis, respectively. Plasma levels of the organ damage markers were analyzed at the IDEXX laboratories (North Grafton, MA). Livers were fixed in 10% neutral buffered formalin, and all liver lobes were sectioned longitudinally for routine histopathological processing and H&E staining. Liver pathology was assessed and semi-quantified in a blinded fashion by a board-certified veterinary pathologist (S.M). The liver was scored for inflammation, hepatocellular degeneration, hepatocellular necrosis, and vascular congestion on a scale of 0 to 4 (none, minimal, mild, moderate, and severe/marked, respectively). The presence of fibrin thrombi or other tissue alterations, if any, were also noted.

**CFU counting**—Liver and spleen were harvested in 500  $\mu$ L sterile PBS containing protease inhibitor 3 days post-infection with 10<sup>3</sup> CFU of *B. thailandensis*. Organs were

homogenized and serially diluted before plating on LB agar plates. Plates were incubated for 48 h at 37°C before CFU counting.

## QUANTIFICATION AND STATISTICAL ANALYSIS

Data were analyzed for statistical significance by unpaired two-tailed t test or one-way ANOVA, as indicated in the legends with Prism software. P values of < 0.05 were considered significant (\*p < 0.05; \*\*p < 0.01; \*\*\*p < 0.001, \*\*\*\*p < 0.0001). Kaplan and Meier survival curves were compared using the log-rank (Mantel-Cox) test, and the adjusted p values for multiple comparisons were shown. The statistical details are provided in the figure legends.

## Supplementary Material

Refer to Web version on PubMed Central for supplementary material.

## ACKNOWLEDGMENTS

We thank Drs. Vishva Dixit and Kate Fitzgerald for *Casp11<sup>-/-</sup>* and *Casp11<sup>fl/fl</sup>* mice, and Dr. Ed Miao for *B. thailandensis*. This work was supported by the NIH (R01 AI119015, R21 AI135528, and R01 AI148491 to V.A.R.).

## REFERENCES

- Aachoui Y, Leaf IA, Hagar JA, Fontana MF, Campos CG, Zak DE, Tan MH, Cotter PA, Vance RE, Aderem A, and Miao EA (2013). Caspase-11 protects against bacteria that escape the vacuole. *Science* 339, 975–978. [PubMed: 23348507]
- Aachoui Y, Kajiwarra Y, Leaf IA, Mao D, Ting JP-Y, Coers J, Aderem A, Buxbaum JD, and Miao EA (2015). Canonical Inflammasomes Drive IFN- $\gamma$  to Prime Caspase-11 in Defense against a Cytosol-Invasive Bacterium. *Cell Host Microbe* 18, 320–332. [PubMed: 26320999]
- Abram CL, Roberge GL, Hu Y, and Lowell CA (2014). Comparative analysis of the efficiency and specificity of myeloid-Cre deleting strains using ROSA-EYFP reporter mice. *J. Immunol. Methods* 408, 89–100. [PubMed: 24857755]
- Banerjee I, Behl B, Mendonca M, Shrivastava G, Russo AJ, Menoret A, Ghosh A, Vella AT, Vanaja SK, Sarkar SN, et al. (2018). Gasdermin D Restrains Type I Interferon Response to Cytosolic DNA by Disrupting Ionic Homeostasis. *Immunity* 49, 413–426.e5. [PubMed: 30170814]
- Chen KW, Groß CJ, Sotomayor FV, Stacey KJ, Tschopp J, Sweet MJ, and Schroder K (2014). The neutrophil NLRP4 inflammasome selectively promotes IL-1 $\beta$  maturation without pyroptosis during acute Salmonella challenge. *Cell Rep.* 8, 570–582. [PubMed: 25043180]
- Chen KW, Monteleone M, Boucher D, Sollberger G, Ramnath D, Condon ND, von Pein JB, Broz P, Sweet MJ, and Schroder K (2018). Noncanonical inflammasome signaling elicits gasdermin D-dependent neutrophil extracellular traps. *Sci. Immunol* 3, eaar6676. [PubMed: 30143554]
- Cheng KT, Xiong S, Ye Z, Hong Z, Di A, Tsang KM, Gao X, An S, Mittal M, Vogel SM, et al. (2017). Caspase-11-mediated endothelial pyroptosis underlies endotoxemia-induced lung injury. *J. Clin. Invest* 127, 4124–4135. [PubMed: 28990935]
- Deng M, Tang Y, Li W, Wang X, Zhang R, Zhang X, Zhao X, Liu J, Tang C, Liu Z, et al. (2018). The Endotoxin Delivery Protein HMGB1 Mediates Caspase-11-Dependent Lethality in Sepsis. *Immunity* 49, 740–753.e7. [PubMed: 30314759]
- Fang R, Uchiyama R, Sakai S, Hara H, Tsutsui H, Suda T, Mitsuyama M, Kawamura I, and Tsuchiya K (2019). ASC and NLRP3 maintain innate immune homeostasis in the airway through an inflammasome-independent mechanism. *Mucosal Immunol.* 12, 1092–1103. [PubMed: 31278375]
- Flood B, Manils J, Nulty C, Flis E, Kenealy S, Barber G, Fay J, Mills KHG, Kay EW, and Creagh EM (2019). Caspase-11 regulates the tumour suppressor function of STAT1 in a murine model of colitis-associated carcinogenesis. *Oncogene* 38, 2658–2674. [PubMed: 30538296]

- Hagar JA, Powell DA, Aachoui Y, Ernst RK, and Miao EA (2013). Cytoplasmic LPS activates caspase-11: implications in TLR4-independent endotoxic shock. *Science* 341, 1250–1253. [PubMed: 24031018]
- He WT, Wan H, Hu L, Chen P, Wang X, Huang Z, Yang Z-H, Zhong C-Q, and Han J (2015). Gasdermin D is an executor of pyroptosis and required for interleukin-1 $\beta$  secretion. *Cell Res.* 25, 1285–1298. [PubMed: 26611636]
- Karmakar M, Minns M, Greenberg EN, Diaz-Aponte J, Pestonjamas K, Johnson JL, Rathkey JK, Abbott DW, Wang K, Shao F, et al. (2020). N-GSDMD trafficking to neutrophil organelles facilitates IL-1 $\beta$  release independently of plasma membrane pores and pyroptosis. *Nat. Commun* 11, 2212. [PubMed: 32371889]
- Kayagaki N, Warming S, Lamkanfi M, Vande Walle L, Louie S, Dong J, Newton K, Qu Y, Liu J, Heldens S, et al. (2011). Non-canonical inflammasome activation targets caspase-11. *Nature* 479, 117–121. [PubMed: 22002608]
- Kayagaki N, Wong MT, Stowe IB, Ramani SR, Gonzalez LC, Akashi-Takamura S, Miyake K, Zhang J, Lee WP, Muszyski A, et al. (2013). Noncanonical inflammasome activation by intracellular LPS independent of TLR4. *Science* 341, 1246–1249. [PubMed: 23887873]
- Kayagaki N, Stowe IB, Lee BL, O'Rourke K, Anderson K, Warming S, Cuellar T, Haley B, Roose-Girma M, Phung QT, et al. (2015). Caspase-11 cleaves gasdermin D for non-canonical inflammasome signalling. *Nature* 526, 666–671. [PubMed: 26375259]
- Knodler LA, Crowley SM, Sham HP, Yang H, Wrangle M, Ma C, Ernst RK, Steele-Mortimer O, Celli J, and Vallance BA (2014). Noncanonical inflammasome activation of caspase-4/caspase-11 mediates epithelial defenses against enteric bacterial pathogens. *Cell Host Microbe* 16, 249–256. [PubMed: 25121752]
- Kovacs SB, Oh C, Maltez VI, McGlaughon BD, Verma A, Miao EA, and Aachoui Y (2020). Neutrophil Caspase-11 Is Essential to Defend against a Cytosol-Invasive Bacterium. *Cell Rep.* 32, 107967. [PubMed: 32726630]
- Liu Z, Zaki MH, Vogel P, Gurung P, Finlay BB, Deng W, Lamkanfi M, and Kanneganti TD (2012). Role of inflammasomes in host defense against *Citrobacter rodentium* infection. *J. Biol. Chem* 287, 16955–16964. [PubMed: 22461621]
- Liu X, Zhang Z, Ruan J, Pan Y, Magupalli VG, Wu H, and Lieberman J (2016). Inflammasome-activated gasdermin D causes pyroptosis by forming membrane pores. *Nature* 535, 153–158. [PubMed: 27383986]
- Mandal P, Feng Y, Lyons JD, Berger SB, Otani S, DeLaney A, Tharp GK, Maner-Smith K, Burd EM, Schaeffer M, et al. (2018). Caspase-8 Collaborates with Caspase-11 to Drive Tissue Damage and Execution of Endotoxic Shock. *Immunity* 49, 42–55.e6. [PubMed: 30021146]
- Mankan AK, Dau T, Jenne D, and Hornung V (2012). The NLRP3/ASC/Caspase-1 axis regulates IL-1 $\beta$  processing in neutrophils. *Eur. J. Immunol* 42, 710–715. [PubMed: 22213227]
- Nichols RD, von Moltke J, and Vance RE (2017). NAIP/NLRC4 inflammasome activation in MRP8<sup>+</sup> cells is sufficient to cause systemic inflammatory disease. *Nat. Commun* 8, 2209. [PubMed: 29263322]
- Rathinam VAK, Zhao Y, and Shao F (2019). Innate immunity to intracellular LPS. *Nat. Immunol* 20, 527–533. [PubMed: 30962589]
- Rühl S, and Broz P (2015). Caspase-11 activates a canonical NLRP3 inflammasome by promoting K(+) efflux. *Eur. J. Immunol* 45, 2927–2936. [PubMed: 26173909]
- Rühl S, Shkarina K, Demarco B, Heilig R, Santos JC, and Broz P (2018). ESCRT-dependent membrane repair negatively regulates pyroptosis downstream of GSDMD activation. *Science* 362, 956–960. [PubMed: 30467171]
- Russo AJ, Behl B, Banerjee I, and Rathinam VAK (2018). Emerging Insights into Noncanonical Inflammasome Recognition of Microbes. *J. Mol. Biol* 430, 207–216. [PubMed: 29017836]
- Russo AJ, Vasudevan SO, Méndez-Huergo SP, Kumari P, Menoret A, Duduskar S, Wang C, Pérez Sáez JM, Fettis MM, Li C, et al. (2021). Intracellular immune sensing promotes inflammation via gasdermin D-driven release of a lectin alarmin. *Nat. Immunol* 22, 154–165. [PubMed: 33398185]

- Schmid-Burgk JL, Gaidt MM, Schmidt T, Ebert TS, Bartok E, and Hornung V (2015). Caspase-4 mediates non-canonical activation of the NLRP3 inflammasome in human myeloid cells. *Eur. J. Immunol* 45, 2911–2917. [PubMed: 26174085]
- Shi J, Zhao Y, Wang Y, Gao W, Ding J, Li P, Hu L, and Shao F (2014). Inflammatory caspases are innate immune receptors for intracellular LPS. *Nature* 514, 187–192. [PubMed: 25119034]
- Shi J, Zhao Y, Wang K, Shi X, Wang Y, Huang H, Zhuang Y, Cai T, Wang F, and Shao F (2015). Cleavage of GSDMD by inflammatory caspases determines pyroptotic cell death. *Nature* 526, 660–665. [PubMed: 26375003]
- Snyder AG, and Oberst A (2021). The Antisocial Network: Cross Talk Between Cell Death Programs in Host Defense. *Annu. Rev. Immunol* 39, 1–25. [PubMed: 33902314]
- Sollberger G, Choidas A, Burn GL, Habenberger P, Di Lucrezia R, Kordes S, Menninger S, Eickhoff J, Nussbaumer P, Klebl B, et al. (2018). Gasdermin D plays a vital role in the generation of neutrophil extracellular traps. *Sci. Immunol* 3, eaar6689. [PubMed: 30143555]
- Vanaja SK, Russo AJ, Behl B, Banerjee I, Yankova M, Deshmukh SD, and Rathinam VAK (2016). Bacterial Outer Membrane Vesicles Mediate Cytosolic Localization of LPS and Caspase-11 Activation. *Cell* 165, 1106–1119. [PubMed: 27156449]
- Wang J, Shao Y, Wang W, Li S, Xin N, Xie F, and Zhao C (2017a). Caspase-11 deficiency impairs neutrophil recruitment and bacterial clearance in the early stage of pulmonary *Klebsiella pneumoniae* infection. *Int. J. Med. Microbiol* 307, 490–496. [PubMed: 28939441]
- Wang W, Shao Y, Li S, Xin N, Ma T, Zhao C, and Song M (2017b). Caspase-11 Plays a Protective Role in Pulmonary *Acinetobacter baumannii* Infection. *Infect. Immun* 85, e00350–17. [PubMed: 28760936]
- Wang J, Sahoo M, Lantier L, Warawa J, Cordero H, Deobald K, and Re F (2018). Caspase-11-dependent pyroptosis of lung epithelial cells protects from melioidosis while caspase-1 mediates macrophage pyroptosis and production of IL-18. *PLoS Pathog.* 14, e1007105. [PubMed: 29791511]
- Wang J, Deobald K, and Re F (2019). Gasdermin D Protects from Melioidosis through Pyroptosis and Direct Killing of Bacteria. *J. Immunol* 202, 3468–3473. [PubMed: 31036765]
- Wiersinga WJ, van der Poll T, White NJ, Day NP, and Peacock SJ (2006). Melioidosis: insights into the pathogenicity of *Burkholderia pseudomallei*. *Nat. Rev. Microbiol* 4, 272–282. [PubMed: 16541135]
- Wu C, Lu W, Zhang Y, Zhang G, Shi X, Hisada Y, Grover SP, Zhang X, Li L, Xiang B, et al. (2019). Inflammasome Activation Triggers Blood Clotting and Host Death through Pyroptosis. *Immunity* 50, 1401–1411.e4. [PubMed: 31076358]
- Yang X, Cheng X, Tang Y, Qiu X, Wang Y, Kang H, Wu J, Wang Z, Liu Y, Chen F, et al. (2019). Bacterial Endotoxin Activates the Coagulation Cascade through Gasdermin D-Dependent Phosphatidylserine Exposure. *Immunity* 51, 983–996.e6. [PubMed: 31836429]
- Zanoni I, Tan Y, Di Gioia M, Broggi A, Ruan J, Shi J, Donado CA, Shao F, Wu H, Springstead JR, and Kagan JC (2016). An endogenous caspase-11 ligand elicits interleukin-1 release from living dendritic cells. *Science* 352, 1232–1236. [PubMed: 27103670]

**Highlights**

- Macrophage/monocyte-specific caspase-11 plays a dominant detrimental role in sepsis
- DC- and intestinal epithelial cell-specific caspase-11 play minor roles in sepsis
- Neutrophil-specific caspase-11 is dispensable for lethal LPS shock
- Macrophage- and neutrophil-specific caspase-11 confer antibacterial defense

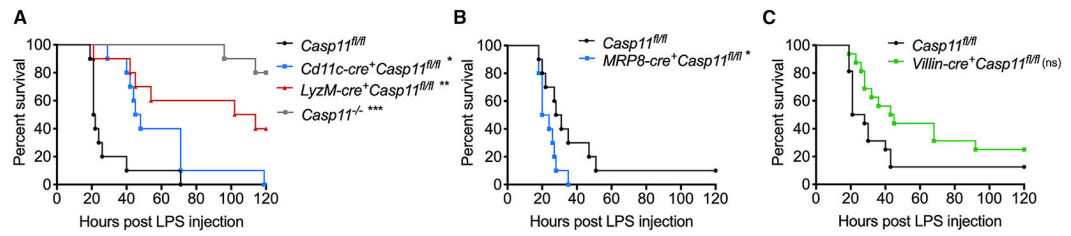


**Figure 1. Cell-type-specific role of caspase-11 in LPS-induced lethality**

(A) Survival of *Casp11<sup>fl/fl</sup>* (n = 10), *Cd11c-cre<sup>+</sup>Casp11<sup>fl/fl</sup>* (n = 10), *LyzM-cre<sup>+</sup>Casp11<sup>fl/fl</sup>* (n = 10), and *Casp11<sup>-/-</sup>* mice (n = 10) injected intraperitoneally (i.p.) with 20 mg/kg LPS.

(B) Survival of *Casp11<sup>fl/fl</sup>* (n = 10) and *MRP8-cre<sup>+</sup>Casp11<sup>fl/fl</sup>* mice (n = 10) injected i.p. with 20 mg/kg LPS.

(C) Survival of *Casp11<sup>fl/fl</sup>* (n = 16) and *Villin-cre<sup>+</sup>Casp11<sup>fl/fl</sup>* mice (n = 16) injected i.p. with 20 mg/kg LPS.

Combined data from two (A and B) or three (C) independent experiments are shown.

Adjusted \*p 0.0166, \*\*p 0.003, and \*\*\*p 0.0003, respectively, for *Casp11<sup>fl/fl</sup>* versus the respective group (Mantel-Cox test). ns, not significant.

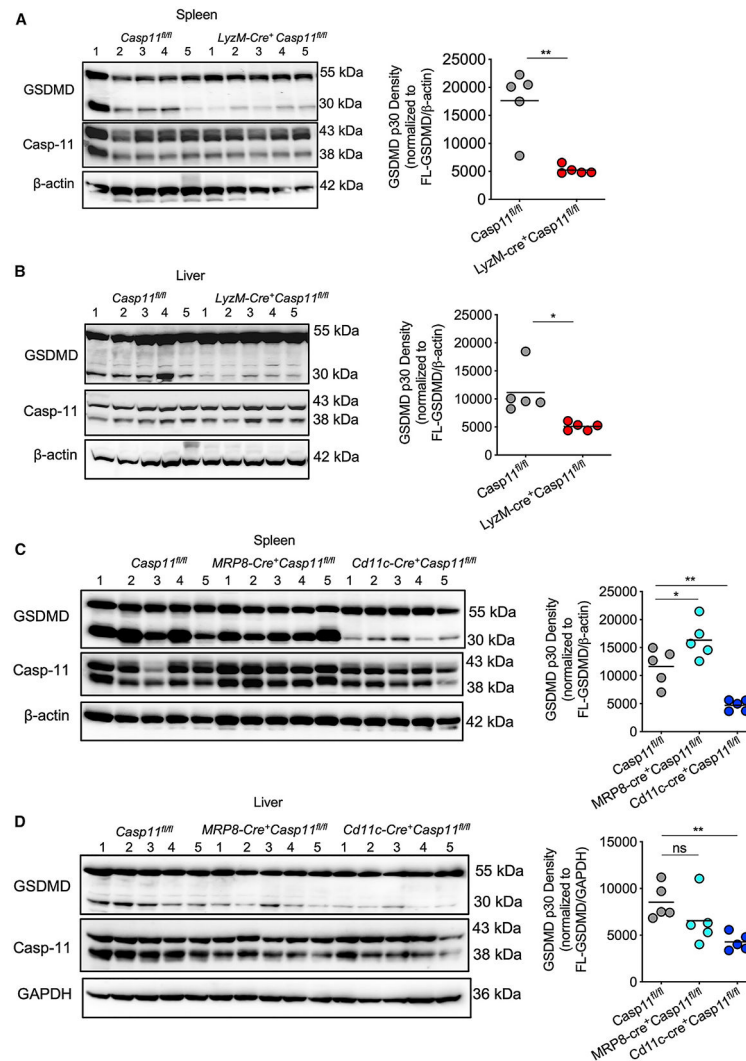


**Figure 2. Cell-type-specific role of caspase-11 in GSDMD activation in tissues during LPS shock** (A and B) Immunoblots of GSDMD, caspase-11, and  $\beta$ -Actin in the lysates of the spleen (A) and liver (B) of *Casp11<sup>fl/fl</sup>* ( $n = 5$ ) and *LyzM-cre<sup>+</sup>Casp11<sup>fl/fl</sup>* mice ( $n = 5$ ) injected with 20 mg/kg LPS for 8 h. Densitometric analysis of cleaved N-terminal fragment of GSDMD (p30) normalized to full-length GSDMD (FL-GSDMD) and  $\beta$ -Actin is shown on the right. (C and D) Immunoblots of GSDMD, caspase-11, and  $\beta$ -Actin in the lysates of the spleen (C) and GSDMD, caspase-11, and GAPDH in the lysates of the liver (D) of *Casp11<sup>fl/fl</sup>* ( $n = 5$ ), *MRP8-cre<sup>+</sup>Casp11<sup>fl/fl</sup>* ( $n = 5$ ), and *Cd11c-cre<sup>+</sup>Casp11<sup>fl/fl</sup>* mice ( $n = 5$ ) injected with 20 mg/kg LPS for 8 h. Densitometric analysis of cleaved N-terminal fragment of GSDMD (p30) normalized to full-length GSDMD and  $\beta$ -Actin or GAPDH is shown on the right. Results shown are representative of two independent experiments. Each circle represents a mouse, and the horizontal lines represent the mean. \* $p < 0.05$ ; \*\* $p < 0.01$ ; unpaired two-tailed t test (A and B) and one-way ANOVA followed by Sidak's post-test (C and D). See also Figures S1-S3.

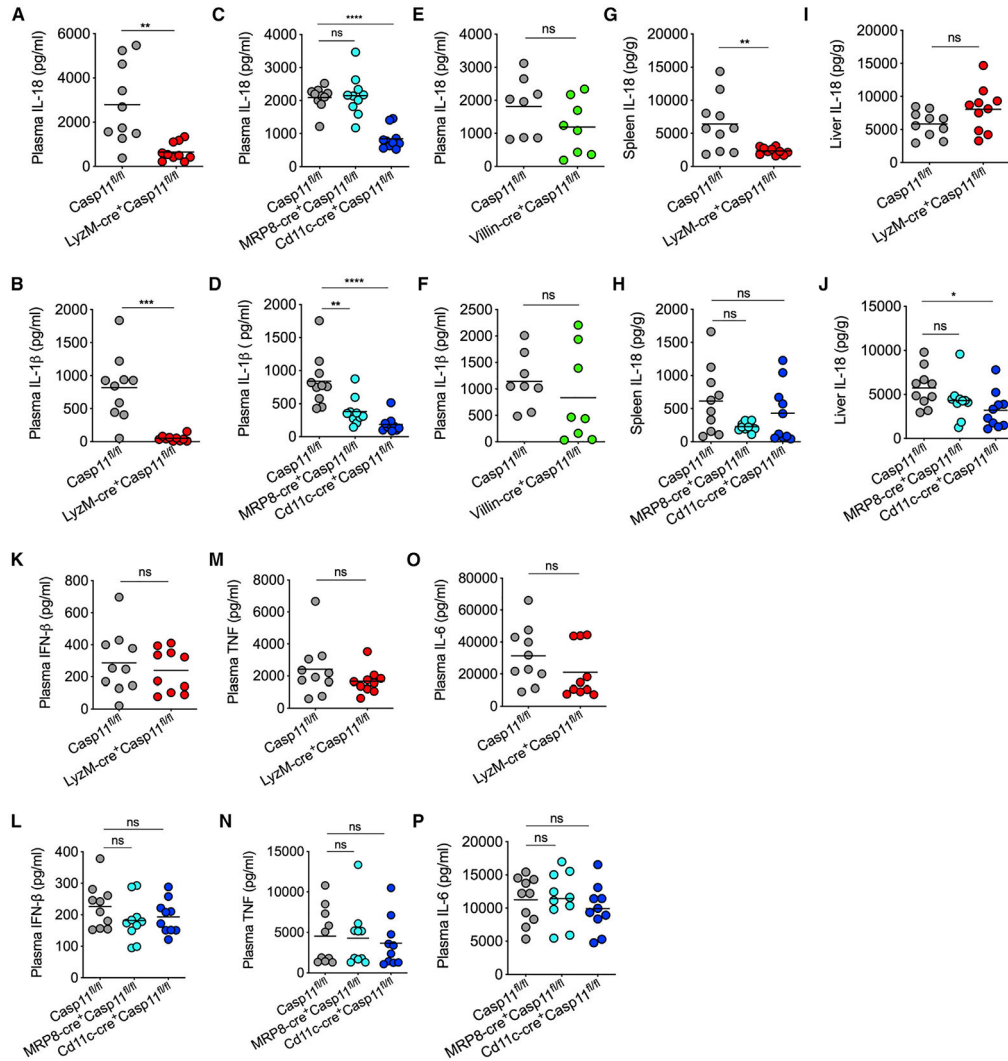


**Figure 3. Cell type-specific role of caspase-11 in IL-18 and IL-1β activation during endotoxemia** (A–F) IL-18 and IL-1β amounts in the plasma of indicated mice 8 h post-LPS injection (20 mg/kg). (G–J) IL-18 amounts in the spleen and liver of indicated mice 8 h post-LPS injection (20 mg/kg). (K–P) IFN-β, TNF, and IL-6 amounts in the plasma of indicated mice 8 h post-LPS injection (20 mg/kg). Combined data from two independent experiments are shown. Each circle represents a mouse, and the horizontal lines represent the mean. \*p < 0.05; \*\*p < 0.01; \*\*\*p < 0.001; \*\*\*\*p < 0.0001; unpaired two-tailed t test (A, B, E–G, I, K, M, and O) and one-way ANOVA followed by Sidak’s post-test (C, D, H, J, L, N, and P). See also Figures S2 and S3.

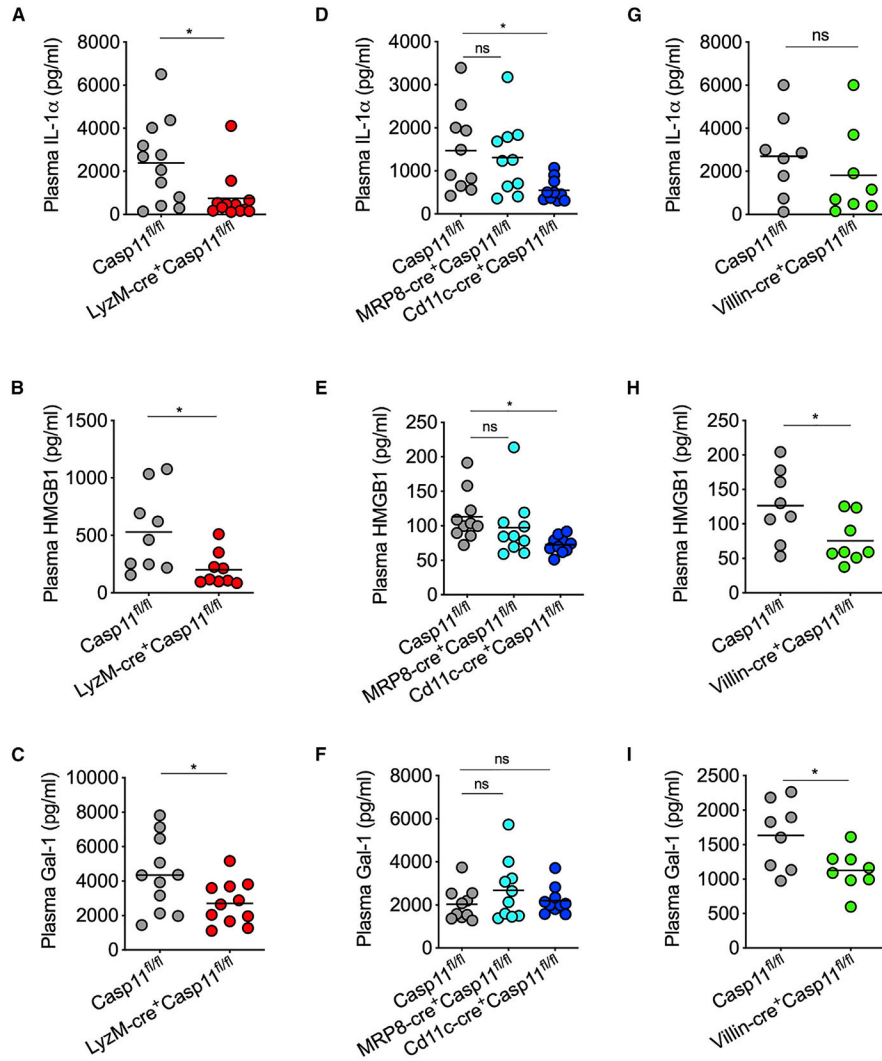


**Figure 4. Cell-type-specific role of caspase-11 in the release of DAMPs/alarmins during endotoxemia**

IL-1α, HMGB1, and galectin-1 amounts in the plasma of (A–C) *Casp11<sup>fl/fl</sup>* and *LyzM-cre<sup>+</sup>Casp11<sup>fl/fl</sup>* mice; (D–F) *Casp11<sup>fl/fl</sup>*, *MRP8-cre<sup>+</sup>Casp11<sup>fl/fl</sup>*, and *Cd11c-cre<sup>+</sup>Casp11<sup>fl/fl</sup>* mice; and (G–I) *Casp11<sup>fl/fl</sup>* and *Villin-cre<sup>+</sup>Casp11<sup>fl/fl</sup>* mice 8 h post-LPS injection (20 mg/kg).

Combined data from two independent experiments are shown. Each circle represents a mouse, and the horizontal lines represent the mean. \*p < 0.05; unpaired two-tailed t test (A–C and G–I) and one-way ANOVA followed by Sidak's post-test (D–F).

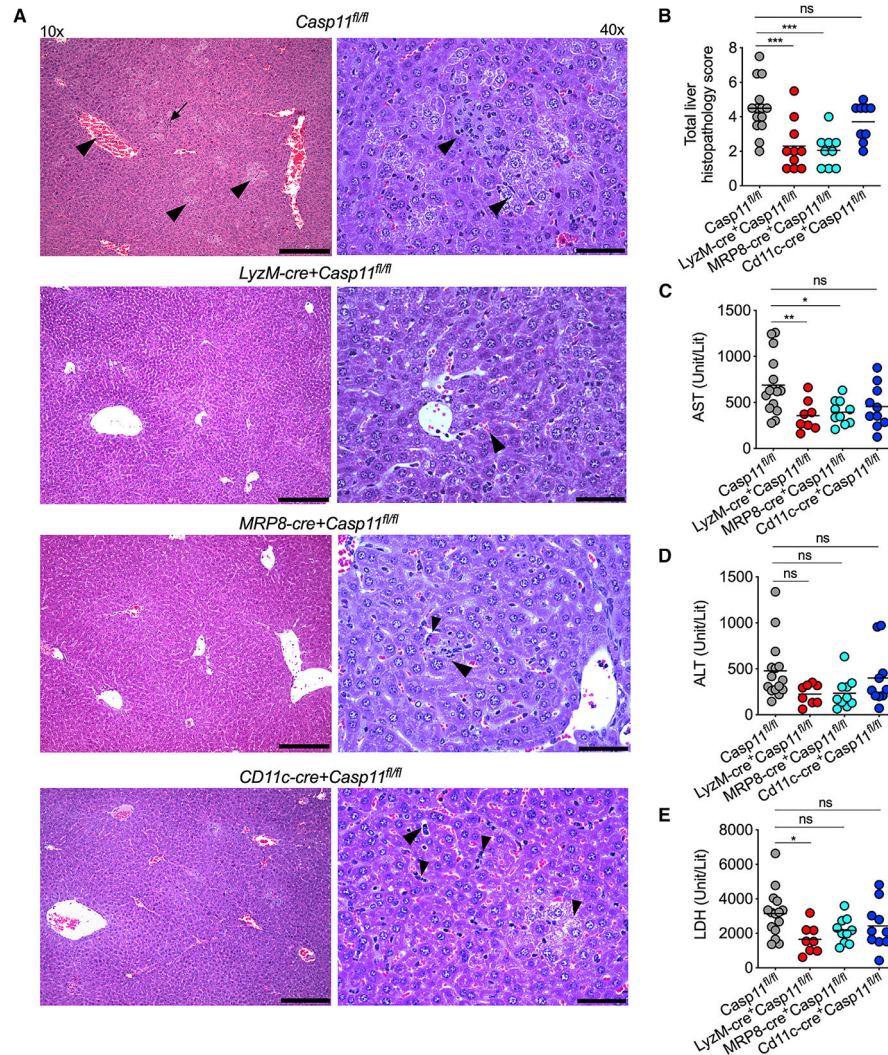


**Figure 5. Cell-type-specific role of caspase-11 in tissue damage during LPS shock**  
 (A and B) Histopathology images (A) of H&E-stained liver sections from *Casp11<sup>fl/fl</sup>*, *LyzM-cre<sup>+</sup>Casp11<sup>fl/fl</sup>*, *MRP8-cre<sup>+</sup>Casp11<sup>fl/fl</sup>*, and *Cd11c-cre<sup>+</sup>Casp11<sup>fl/fl</sup>* mice 16 h post-LPS injection (20 mg/kg) and the corresponding histopathological scoring (B). Representative images for each genotype are shown. Histopathological lesions such as hepatocellular degeneration/necrosis, venous/sinusoidal congestion, or inflammatory cell infiltrates are indicated by arrowheads and inflammatory foci with necrosis by the arrow. Scale bars represent 250  $\mu$ M (10 $\times$ ) and 60  $\mu$ M (40 $\times$ ).  
 (C–E) AST, ALT, and LDH amounts in the plasma of indicated mice 16 h post-LPS injection (20 mg/kg).  
 Each circle represents a mouse, and the horizontal lines represent mean. \* $p < 0.05$ ; \*\* $p < 0.01$ ; \*\*\* $p < 0.001$ ; one-way ANOVA followed by Sidak's post-test (B–E). See also Figure S4.

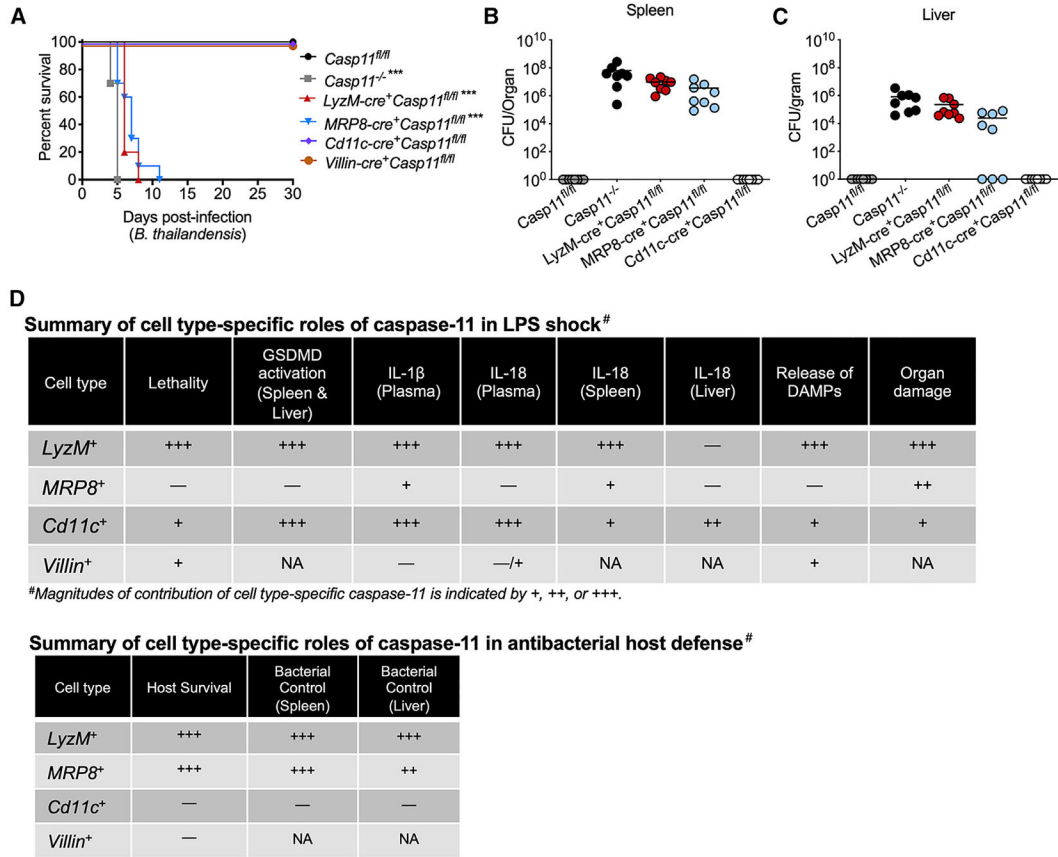


**Figure 6. Cell-type-specific role of caspase-11 in antibacterial host defense**

(A) Survival of *Casp11<sup>fl/fl</sup>* (n = 8), *Casp11<sup>-/-</sup>* (n = 8), *LyzM-cre<sup>+</sup>Casp11<sup>fl/fl</sup>* (n = 8), *MRP8-cre<sup>+</sup>Casp11<sup>fl/fl</sup>* (n = 8), *Cd11c-cre<sup>+</sup>Casp11<sup>fl/fl</sup>* (n = 8), and *Villin-cre<sup>+</sup>Casp11<sup>fl/fl</sup>* mice (n = 8) infected i.p. with *B. thailandensis* ( $10^3$  CFUs).

(B and C) Bacterial loads in the spleen (B) and liver (C) of *Casp11<sup>fl/fl</sup>* (n = 8), *Casp11<sup>-/-</sup>* (n = 8), *LyzM-cre<sup>+</sup>Casp11<sup>fl/fl</sup>* (n = 8), *MRP8-cre<sup>+</sup>Casp11<sup>fl/fl</sup>* (n = 8), and *Cd11c-cre<sup>+</sup>Casp11<sup>fl/fl</sup>* mice (n = 8) infected i.p. with *B. thailandensis* ( $10^3$  CFUs) on 3 days post-infection. Data from two independent experiments are shown. Each circle represents a mouse, and the horizontal lines represent the mean.

(D) Summary of cell-type-specific roles of cytosolic LPS sensing in LPS shock and antibacterial host defense against *B. thailandensis*. Plus sign (+) indicates the magnitude of contribution (+++ and + indicate strong and weak contributions, respectively); —, no role; NA, not assessed. \*\*\*p < 0.0002 (adjusted p value; Mantel-Cox test).

## KEY RESOURCES TABLE

REAGENT or RESOURCE	SOURCE	IDENTIFIER
<b>Antibodies</b>		
Mouse monoclonal Anti mouse $\beta$ -actin (Clone 8H10D10)	Cell Signaling Technology	Cat# 3700; RRID:AB_2242334
Rabbit monoclonal Anti-mouse GSDMD (Clone EPR 19828)	Abcam	Cat# Ab209845; RRID:AB_2783550
Rat monoclonal Anti-mouse Caspase 11 (Clone 17D9)	Cell Signaling Technology	Cat# 14340S; RRID:AB_2728693
Rabbit monoclonal Anti-mouse MLKL (Clone D6W1K)	Cell Signaling Technology	Cat# 3770S; RRID:AB_2799118
Rabbit monoclonal Anti-mouse pMLKL (Ser345) (Clone D6E3G)	Cell Signaling Technology	Cat# 37333; RRID:AB_2799112
Rabbit monoclonal Anti-mouse Casp3 (cleaved) (Clone 5A1E)	Cell Signaling Technology	Cat# 9664; RRID:AB_2070042
Rabbit monoclonal Anti-mouse GAPDH (Clone D16H11)	Cell Signaling Technology	Cat# 5174; RRID:AB_10622025
Anti-Rat IgG HRP	Jackson ImmunoResearch Labs	Cat# 712-035-150; RRID:AB_2340638
Anti-Mouse IgG HRP	Jackson ImmunoResearch Labs	Cat# 115-035-166; RRID:AB_2338511
Anti-Rabbit IgG HRP	Jackson ImmunoResearch Labs	Cat# 711-035-152; RRID:AB_10015282
Rat monoclonal anti-IL-18 antibody (Clone#74; ELISA capture antibody)	MBL International	Cat# D047-3; RRID:AB_592016
Rat monoclonal anti-IL-18 antibody Biotin (Clone#93-10C; ELISA detection antibody)	MBL International	Cat# D048-6; RRID:AB_592012
Rat monoclonal anti-IFN- $\beta$ antibody (7F-D3; ELISA capture antibody)	Santa Cruz Biotechnology	Cat# sc-57201; RRID:AB_2122911
Rabbit polyclonal anti-IFN- $\beta$ antibody (ELISA detection antibody)	PBL	Cat# 32400-1; RRID:AB_387872
APC-anti-mouse/human CD11b antibody	BioLegend	Cat# 101212; RRID:AB_312795
<u>PE/Cyanine7 anti-mouse CD11c antibody</u>	BioLegend	Cat# 117318; RRID:AB_493568
PerCP/Cyanine5.5 anti-mouse Ly6C antibody	BioLegend	Cat# 128012; RRID:AB_1659241
Pacific Blue anti-mouse Ly6G antibody	BioLegend	Cat# 127612; RRID:AB_2251161
PE anti-mouse F4/80 antibody	BioLegend	Cat# 123110; RRID:AB_893486
Alexa Fluor 700 anti-mouse/human CD45R/B220 antibody	BioLegend	Cat# 103232; RRID:AB_493717
Alexa Fluor 700 anti-mouse CD3epsilon antibody	BioLegend	Cat# 152316; RRID:AB_2632713
Live/Dead Fixable Dead cell stain kit	Invitrogen	Cat# L34962
<b>Bacterial and virus strains</b>		
<i>Burkholderia thailandensis</i>	Aachoui et al. (2015), Cell Host Microbe	E264-1
<b>Chemicals, peptides, and recombinant proteins</b>		
LPS E.coli O111:B4	Sigma	Cat# L3024-25MG
Recombinant Mouse IFN- $\beta$ (for ELISA)	BioLegend	Cat# 581302
Collagenase	Sigma Aldrich	Cat# C5138-5G
DNaseI	Sigma Aldrich	Cat# DN25-1G
<b>Critical commercial assays</b>		
Mouse IL-1 $\beta$ ELISA kit	Thermo Fisher Scientific	Cat# 50-171-85
Mouse IL-6 ELISA kit	Thermo Fisher Scientific	Cat# 50-172-18
Mouse TNF ELISA kit	Thermo Fisher Scientific	Cat# 88-7324
Mouse IL-1 $\alpha$ ELISA kit	Thermo Fisher Scientific	Cat# 88-5019
Mouse Galectin-1 ELISA kit	R&D Systems	Cat# DY1245

REAGENT or RESOURCE	SOURCE	IDENTIFIER
Human HMGB1 ELISA kit	IBL International	Cat# ST51011
Pierce™ BCA Protein Assay kit	Thermo Fisher Scientific	Cat# 23227
Halt™ Protease Inhibitor Cocktail (100X)	Thermo Fisher Scientific	Cat# 1861279
NuPAGE LDS sample buffer (4X)	Invitrogen	Cat# NP0007
Trans-Blot Turbo Transfer System	Bio-Rad	Cat# 1704271
Clarity ECL HRP Substrate	Bio-Rad	Cat# 170-5060S
Experimental models: Organisms/strains		
Mouse: <i>Casp1<sup>fl/fl</sup></i>	Kayagaki et al. (2011), Genentech	N/A
LysM-Cre Mouse: B6.129P2- <i>Lyz2<sup>tm1(cre)Hof</sup>/J</i>	The Jackson Laboratory	IMSR Cat# JAX:004781; RRID:IMSR_JAX:004781
MRP8-Cre Mouse: B6.Cg-Tg(S100A8-cre,-EGFP)1Ilw/J	The Jackson Laboratory	IMSR Cat# JAX:021614; RRID:IMSR_JAX:021614
Cd11c-Cre Mouse: B6.Cg-Tg(Itgax-cre)1-1Reiz/J	The Jackson Laboratory	IMSR Cat# JAX:008068; RRID:IMSR_JAX:008068
Villin-Cre Mouse: B6.Cg-Tg(Vill1-cre)997Gum/J	The Jackson Laboratory	IMSR Cat# JAX:004586; RRID:IMSR_JAX:004586
Mouse: <i>Casp1<sup>-/-</sup></i>	Kayagaki et al. (2011), Genentech	N/A
Oligonucleotides		
1) Primers for <i>Casp1<sup>fl/fl</sup></i> genotyping Primer 1: CCCTGGAAAAATCGATGACT Primer 2: TGAAATGCATGTACTGAGAGCAAGG Primer 3: CAATTGACTTGGGGATTCTGG	Kayagaki et al. (2011), Genentech & Integrated DNA Technologies	Mouse listed above
2) Primers for LysM-Cre detection Primer 1 (Mutant_oIMR3066): CCCAGAAATGCCAGATTACG, Primer 2 (Common_oIMR3067): CTTGGGCTGCCAGAATTTCTC Primer 3 (WT_oIMR3068): TTACAGTCGGCCAGGCTGAC	The Jackson Laboratory & Integrated DNA Technologies	Mouse listed above
3) Primers for MRP8-Cre detection Primer 1 (Cre_Fwd_oIMR1084): GCGGTCTGGCAGTAAAACTATC Primer 2 (Cre_Rev_oIMR1085): GTGAAACAGCATTGCTGTCACCT Primer 3 (Internal_Fwd_oIMR7338): CTAGGCCACAGAATTGAAAGATCT Primer 4 (Internal_Rev_oIMR7339): GTAGGTGGAAATTCTAGCATCATCC	The Jackson Laboratory & Integrated DNA Technologies	Mouse listed above
4) Primers for Cd11c-Cre detection Primer 1 (Cre_Fwd_oIMR7841): ACTTGGCAGCTGTCTCCAAG Primer 2 (Cre_Rev_oIMR7842): GCGAACATCTTCAGGTTCTG Primer 3 (Internal_Fwd_oIMR8744): CAAATGTTGCTTGCTGGTG Primer 4 (Internal_Rev_oIMR8745): GTCAGTCGAGTGCACAGTTT	The Jackson Laboratory & Integrated DNA Technologies	Mouse listed above
5) Primers for Villin-Cre detection Primer 1 (Common_40114): GCTTTCAAGTTTCATCCATGTTG Primer 2 (WT_Rev_40115): TTCATGATAGACAGATGAACACAGT Primer 3 (Mutant_Rev_40117): GTCTTTGGGTAAGCCAAGC	The Jackson Laboratory & Integrated DNA Technologies	Mouse listed above
Software and algorithms		
GraphPad Prism 9.0	GraphPad Software	N/A
FlowJo (version 10.7)	Tree Star	N/A
GeneSnap(version 7.12)	Syngene	N/A
Biorender	Biorender	N/A
Fiji/ImageJ (version 10.2)	<a href="https://imagej.net/Fiji">https://imagej.net/Fiji</a>	N/A